A new method for systematic 1-step chemistry reduction applied to hydrocarbon combustion

Alejandro Millán-Merino, Said Taileb, Pierre Boivin

A new method for systematic 1-step chemistry reduction applied to hydrocarbon combustion

Alejandro Millán-Merino*, Said Taileb, Pierre Boivin

Aix Marseille Univ, CNRS, Centrale Marseille, M2P2, Marseille, France

Abstract

We propose a new single-step mechanism for the combustion of arbitrary hydrocarbons and alcohols. Unlike most single-step models, no tabulation is required, as the method builds upon a new analytical description of the thermochemical equilibrium of fuel-oxidizer mixtures including dihydrogen and carbon monoxide – two species usually discarded in one-step descriptions – yielding correct adiabatic temperature. The single-step chemistry includes varying stoichiometric coefficients, ensuring a convergence towards thermochemical equilibrium regardless of the local state. The reaction rate is then carefully adjusted to reproduce accurately premixed flames. To tackle ignition simultaneously, an additional passive scalar advection-diffusion-reaction equation is introduced, with a rate fitted on ignition delays. The scalar then serves as an efficiency to modify the single-step reaction rate in autoignition configurations. The obtained scheme is then validated for a wide range of equivalence ratios on homogeneous reactors, premixed flames, a triple flame, and a counterflow diffusion flame. The new analytical thermochemical equilibrium formulation may also serve in speeding up infinitely fast chemistry calculations.

Keywords: Single-step chemistry; Laminar flame speed; Ignition delay time; Partially premixed combustion; Hydrocarbon combustion

1. Introduction

In modeling combustion chambers, implementation of detailed chemistry is a significant challenge, because both the species number N_s and the number of reactions N_r to be computed can be considerable, e.g. $(N_s, N_r) = (207, 1673)$ for kerosene fuel [1]. Arguably, N_s is most limiting in complex 3D numerical simulations: since simulating the 3D flow requires 5 "mandatory" degrees of freedom (mass, 3× momentum, and energy), considering $N_s = 207$ species comparatively leads to degrees of freedom number increased 40-fold, prohibitive for most complex configurations. On top of that, intermediate species have smaller time scales rendering stiffer the problem.

This explains the abundance in the literature of reduction methods [2–5] and associated simplified descriptions [6–10]. Skeletal descriptions, for instance, consist in identifying and neglecting unim-

* Corresponding author.
E-mail address: almillan@outlook.com (A. Millán-Merino).

portant reactions and species, guided, e.g. by computational singular perturbation [2]. This typically results in mechanisms of a few dozens elementary reactions; e.g. $(N_s, N_r) = (12, 9)$ for H_2 [9], (17,73) for CH_4 [11]. Further reduction is possible through introduction of global reactions (not included in the detailed chemistry descriptions), yielding e.g. $(N_s, N_r) = (5, 3)$ for H_2 [9], $(7, 4)$ for CH_4 [7] or (5,2) for kerosene [8].

In reduced chemistry development, the literature generally agrees on the following two objectives. The first and foremost objective is to accurately reproduce the oxidation heat release, e.g., the burnt gases temperature. This problem is purely a Gibbs energy minimization problem and is therefore independent of the kinetics. In that sense, infinitely fast chemistry schemes are reduced chemistry models that only answer the first objective.

The second objective is to recover a specific set of kinetic properties. These can involve, depending on the model: premixed flame burning velocities [8,12] and thicknesses [4], thermo-acoustic instabilities [13], ignition delays [14–16], temperature in diffusion flames, strain rate at extinction, detonation structures [17], etc.

In tackling the first objective, two main strategies exist. (i) The first is to include in the description the minimal set of species allowing to reach the desired accuracy. For lean premixed hydrocarbons, for instance, considering only the major species (C_nH_m, O_2, CO_2, H_2O) leads to reasonable burnt gas temperatures [4,6]. For most hydrocarbons combustion chambers, however, the mixture is only partially premixed, and albeit lean on average, rich and hot regions can exist and must be carefully treated, as they are, e.g., where soot is produced [18]. It is therefore required to add at least a species (e.g., CO in [8,19]), and a reaction. As noted by Er-raiy et al. [4], H_2 is also required to accurately reproduce burnt temperatures of hydrocarbon-air mixtures, adding yet another species and reaction. (ii) The second strategy consists of altering, one way or another, the heat release or thermodynamic properties controlling the heat release. For instance, Fernández-Tarrazo et al. [6] directly modified the heat release of rich mixtures in the energy equation, while others opted for creating a virtual species for which thermodynamic properties are tabulated from an extensive set of species [4,10].

Regarding the second objective, several options can be found in the literature recovers the kinetic properties. Starting from the detailed chemistry elementary rates, partial-equilibrium and quasi-steady-state approximations are used in fully analytically derived mechanisms [9,20], while more systematic methods study the kinetic source term Jacobian to obtain the main chemical time-scales (see, e.g., [2,3,21]). Very short mechanisms (1–2 steps) tend to resort directly to carefully fitted rates to recover the desired set of kinetic properties [4,10].

In this study, we propose a new method for constructing single-step mechanisms and apply it to CH_4, C_2H_6, C_3H_8, CH_3OH, C_2H_5OH, and kerosene surrogate combustion. Section 2 derives a new asymptotic analysis of the thermodynamic equilibrium, which allows considering a single-step mechanism without appreciable loss of accuracy for the burnt gases temperature in the rich region. The formalism proposed can also drastically reduce the cost of infinitely fast chemistry solvers by avoiding the costly Gibbs energy minimization process. Section 3 introduces a novel method to correct the premixed flame velocity based on a Von-Karman analysis. The method relies only on fitting nine parameters based on detailed chemistry calculations or experimental data, but does not require any tabulation. Section 4 presents a new passive scalar approach based on an eigenvalue study of the Jacobian similar to [2,3,21,22]. The passive scalar serves as an efficiency function in the single-step chemistry and allows to recover ignition characteristics, in addition to partially-premixed phenomena. Section 5 presents additional evaluations, and conclusions are drawn in Section 6. Supplementary Material includes all parameters and validations for CH_4, C_2H_6, C_3H_8, CH_3OH, C_2H_5OH, and a fuel surrogate for kerosene $C_{9.74}H_{20.05}$.

2. Asymptotic analysis of the equilibrium

2.1. Leading order solution

The simplest equilibrium approximation may be obtained by assuming total oxidation:

$$C_nH_m + \left(n + \frac{m}{4}\right)O_2 \xrightarrow{\xi_1} nCO_2 + \frac{m}{2}H_2O. \tag{1}$$

Consider a mixture initially consisting of $n^0_{C_nH_m} = \phi$, and $n^0_{O_2} = n + m/4$, where n^0_i is the initial mole number of the i^{th} species, allowing for ϕ to correspond to the classical equivalence ratio definition

$$\phi = \left(n + \frac{m}{4}\right)\frac{n_{C_nH_m}}{n_{O_2}}. \tag{2}$$

Assuming total oxidation is equivalent to limiting the reaction molar advancement ξ_1 by the deficient reactant as

$$\xi_1 = \min(\phi, 1). \tag{3}$$

From the knowledge of ξ_1, the equilibrium composition is fully characterized. In particular, the burnt gases temperature can be computed from this composition under classical assumptions (e.g., constant pressure and entropy or constant volume and internal energy) [23].

2.2. Recombination reactions extension

Above, we have only assumed that the mixture consists of the principal reactants (C_nH_m, O_2),

products (CO_2, H_2O), and inert gases (e.g., N_2). However, equilibrium properties of hydrocarbon-air blends highly depend on the set of species considered [4,6,8], and it has been corroborated that for typical hydrocarbon-air mixtures at standard conditions at least (CO, H_2) should be taken into account [4]. Their presence can be included by considering the two dissociation reactions

$$CO_2 \xrightarrow{\xi_2} CO + \frac{1}{2}O_2\ ;\ H_2O \xrightarrow{\xi_3} H_2 + \frac{1}{2}O_2. \tag{4}$$

Species mole numbers are related to reaction molar advancement ξ_k as

$$n_i = n_i^0 + \sum_{k=1}^{3} \nu_{k,i}\xi_k \tag{5}$$

with $\nu_{k,i}$ the net stoichiometric coefficient (positive for the products and negative for the reactants) in reaction k. For a complete depletion of C_nH_m, we now obtain

$$\xi_1 = \phi, \quad \xi_{ox} = \xi_2 + \xi_3 = \max(\xi_{ox}^0, 0) \tag{6}$$

with

$$\xi_{ox}^0 = \frac{4n + m}{2}(\phi - 1) \tag{7}$$

being the leading order term in the recombination reaction advancement. Note that in rich conditions, including recombination reactions (4) and associated partially oxidized products CO and H_2, effectively results in the global molar advancement ξ_1 (3) being higher (6). At this stage, there are two options. (i) We can assume a constant value for the relative importance of the recombination reactions (i.e., $\xi_2 = \beta\xi_{ox}$ with β fitted from equilibrium computations), or (ii) take into account the equilibrium constants to compute (ξ_2, ξ_3), as done afterward. Once this is accomplished, ξ_1, ξ_2, and ξ_3 are known, and the equilibrium is fully defined in the same way as in the previous example.

2.3. *Asymptotic correction for ξ_{ox}*

Reminding that exact thermodynamic equilibrium is attained through Gibbs free energy [24]. The total Gibbs free energy of the mixture, G, is minimal when the condition $\partial G/\partial n_i = 0$ is satisfied for each species. Combining the constraints between themselves and with Eq. (5) reaches the equilibrium conditions for the recombination reactions as

$$K_2 = \frac{(n_{CO}^0 + \xi_2)\sqrt{\frac{4n+m}{2}(1-\xi_1) + \xi_{ox}}}{(n_{CO_2}^0 + n\xi_1 - \xi_2)\sqrt{2N^0 + \frac{m-4}{2}\xi_1 + \xi_{ox}}} \tag{8}$$

and

$$K_3 = \frac{(n_{H_2}^0 + \xi_3)\sqrt{\frac{4n+m}{2}(1-\xi_1) + \xi_{ox}}}{(n_{H_2O}^0 + \frac{m}{2}\xi_1 - \xi_3)\sqrt{2N^0 + \frac{m-4}{2}\xi_1 + \xi_{ox}}} \tag{9}$$

with equilibrium constants K_k introduced as

$$K_k = \exp\left(-\sum_{i=1}^{7} \nu_{k,i}\frac{g_i}{\mathcal{R}T}\right)\left(\frac{P^0}{P}\right)^{\sum_{i=1}^{7}\nu_{k,i}}, \tag{10}$$

where g_i is the specific Gibbs energy of the i^{th} species, $\mathcal{R}$ is the ideal gas constant, and P^0 and $N^0 = \sum_{i=1}^{7} n_i^0$ are the reference pressure and the initial mole number concentration. The equilibrium constants are evaluated at the equilibrium temperature and pressure, T and P, respectively. Let us now assume that oxidation reaction 1 is complete ($K_1 \gg 1$) while the two recombination equilibrium constants are small (K_2, K_3) $\ll 1$. At leading order, $K_2 = K_3 = 0$, we recover exactly the solution from Eq. (3) under the same assumptions. For the first correction order, Equations (8) & (9) can be recast as

$$K_{ox} = (\xi_{ox} + n_{ox}^0)\sqrt{\xi_{ox} - \xi_{ox}^0} \tag{11}$$

and

$$K_r = \frac{n_{CO}^0 + \xi_{ox} - \xi_3}{n_{H_2}^0 + \xi_3}\frac{n_{H_2O}^0 + \frac{m}{2}\phi - \xi_3}{n_{CO_2}^0 + n\phi - \xi_{ox} + \xi_3} \tag{12}$$

where the following definitions are introduced for simplicity: $n_{ox}^0 = n_{CO}^0 + n_{H_2}^0$, $K_r = K_2/K_3$, and

$$K_{ox} = \Big[(n_{CO_2}^0 + n\phi)K_2 + \Big(n_{H_2O}^0 + \frac{m}{2}\phi\Big)K_3\Big]\sqrt{2N^0 + \frac{m-4}{2}\phi}. \tag{13}$$

This set of equations is now decoupled and has an explicit solution. The first equation is a third-order polynomial, while the other is a second-order polynomial. The result of Eq. (11) has a single real solution satisfying the physical constraints $\xi_{ox} \geq 0$ and $\xi_{ox} \geq \left(2n + \frac{m}{2}\right)(\phi - 1)$:

$$\xi_{ox} = \frac{\Theta}{3} + \frac{(\xi_{ox}^0 + n_{ox}^0)^2}{3\Theta} + \frac{\xi_{ox}^0 - 2n_{ox}^0}{3} \tag{14}$$

with

$$\Theta = \frac{1}{\sqrt[3]{2}}\sqrt[3]{27K_{ox}^2 + \sqrt{27R_o} + 2(\xi_{ox}^0 + n_{ox}^0)^3} \tag{15}$$

$$R_o = 27K_{ox}^4 + 4K_{ox}^2(\xi_{ox}^0 + n_{ox}^0)^3. \tag{16}$$

These expressions are valid when $R_o \geq 0$, but a similar formula is provided in supplementary material when $R_o < 0$.

For Equation (12), the solution that satisfies the physical description of the problem is

$$\xi_3 = \frac{\sqrt{\mathcal{C}_1^2 + 4(K_r - 1)\mathcal{C}_2} + \mathcal{C}_1}{2(K_r - 1)} \tag{17}$$

with

$$\mathcal{C}_1 = n_{CO}^0 + n_{H_2O}^0 + \xi_{ox} + \frac{m}{2}\phi + \Big(n_{H_2}^0 + n_{CO_2}^0 - \xi_{ox} + n\phi\Big)K_r \tag{18}$$

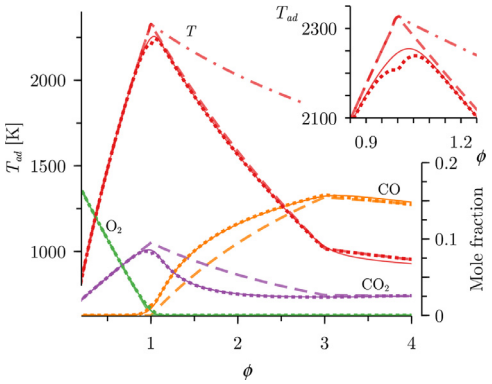

Fig. 1. Adiabatic temperature and equilibrium mole fraction profiles versus the equivalence ratio of methane-air mixtures at constant pressure, $P = 1$bar, and initial gas temperature, $T^0 = 300$K. Solid line: Equilibrium computations with Cantera suite [25] for 7 equilibrium species; Dash-dot line: Leading order solution, Eq. (3) and $\xi_2 = \xi_3 = 0$; Dashed line: Recombination leading order, Eq. (3) with ξ^0_{ox} and $\xi_2 = 0.32\xi^0_{ox}$; Doted line: Recombination asymptotic correction, Eqs. (3), (14), & (17).

$$\mathcal{C}_2 = (n^0_{CO} + \xi_{ox})(n^0_{H_2O} + \frac{m}{2}\phi) - n^0_{H_2}(n^0_{CO_2} - \xi_{ox} + n\phi)K_r. \quad (19)$$

The equilibrium composition (ξ_1, ξ_2, ξ_3) is now defined explicitly through Eqs. (3), (14), & (17). Note, however, that an equilibrium temperature estimate is still required to compute the equilibrium constants (10). In the following, we use the value of T obtained from the simplified problem of Section 2.2, in order to keep the formulation fully explicit. It should be remarked that a higher accuracy may be achieved through a limited number of iterations.

Equilibrium properties of methane-air flame obtained with the present method are compared in Fig. 1 with constant pressure equilibrium computations made with the Cantera suite [25] using 7 equilibrium species. Excellent accuracy is achieved for temperature values when recombination equations are used. For mole fraction profiles, it is clear that the asymptotic correction provides a better agreement with the reference capturing the correct dependency with the equivalence ratio, even in the vicinity of stoichiometry.

Note that a similar agreement is obtained for C_2H_6, C_3H_8, and kerosene $C_{9.74}H_{20.05}$.

2.4. Extension to partially-oxygenated hydrocarbons

The derivation provided in Supplementary material shows that the present work can be extended to arbitrary partially oxygenated hydrocarbon $C_nH_mO_p$ (including, e.g. alcohols C_nH_mOH), through minor modifications of Eqs. (7), (8), (9), and (13). For instance, Eq. (7) becomes

$$\xi^0_{ox} = \frac{4n + m - 2p}{2}(\phi - 1), \quad (20)$$

where p is the number of O-atoms in $C_nH_mO_p$. Results for methanol and ethanol are included throughout the manuscript, showing the same level of agreement as for pure hydrocarbons.

3. Kinetic mechanism

Let us now define a one-step mechanism as

$$\phi C_nH_m + \alpha n^0_{O_2} O_2 \xrightarrow{\omega} n_{CO_2}CO_2 + n_{H_2O}H_2O + n_{CO}CO + n_{H_2}H_2, \quad (21)$$

where $\alpha = (n^0_{O_2} - n_{O_2})/n^0_{O_2}$ is the oxygen ratio consumption and n_i are the stoichiometric coefficients chosen to match the equilibrium calculated in Section 2, taking the local pressure and enthalpy to estimate the equilibrium constants (10).

From this definition, it is clear that no matter the reaction rate, the mixture composition will tend towards the equilibrium composition, allowing for an accurate value of T_b. This strategy avoids the need to define a virtual species with ad-hoc thermodynamic parameters [4,10]. Next, let us introduce a general reaction rate for the global reaction (21) as

$$\omega = C^{s_F}_{C_nH_m} C^{s_O}_{O_2} K \text{ with } K = Be^{-\frac{T_a}{T}}, \quad (22)$$

where reaction exponents (s_F and s_O), pre-exponential factor B and activation temperature T_a are constant to be defined hereafter.

As pointed out by Franzelli et al. [8], there exists a direct relation between the laminar flame velocity V_L pressure dependence $V_L(P) = V_L(P_0)(P/P_0)^\gamma$ and the global order of the reaction through $s = s_F + s_O = 2(\gamma + 1)$. Having defined s from this relation based on detailed chemistry results, we then set on trial and error basis $s_F = s_O = s/2$. Following the strategy of [4,6,8,10], (B, T_a) are then fitted to obtain accurate laminar flame velocity predictions in the lean limit. Results obtained for methane/air mixtures are $B = 1.04 \times 10^8$mol/s cm^3, $T_a = 11070$K, and $s = 1.12$ and they are reproduced in Fig. 2, labeled 1-step N.C.

Comparing the obtained results with the reference solution, it is clear that V_L is overestimated by the single-step mechanism. Since the global reaction (21) is complete, we may adapt the classical asymptotic solution of Zeldovich, Frank-Kamenetskii, and von Karman to the reaction rate (22) as

$$V_L^2 = 2\Gamma(s+1)\left(n + \frac{m}{4}\right)^s \left(\frac{T_b}{T_b - T_u}\right)^{s+1} \frac{\rho_b^s}{\rho_u^2}\frac{\lambda}{c_p}\left(\frac{T_b}{T_a}\right)^{s+1} Be^{-\frac{T_a}{T_b}} \left(\frac{\phi}{n^0_{O_2}}\right)^{s_F} \quad (23)$$

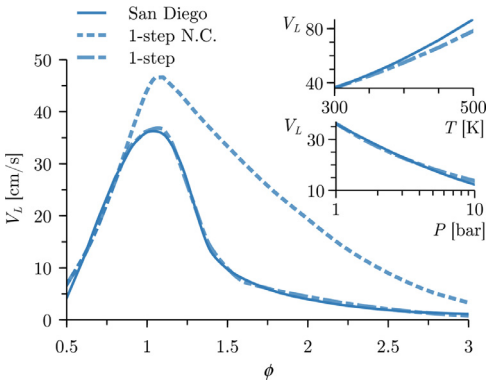

Fig. 2. Laminar flame velocity versus equivalence ratio for methane-air mixtures at initial conditions $T = 300$K and $P = 1$bar. Inset plots represent V_L variations with initial conditions, T and P, for stoichiometric mixtures. Solid line: San Diego mechanism [26], Dashed line: single-step mechanism without correction function, Dot-dash line: present mechanism with the function correction, $\mathcal{F}$.

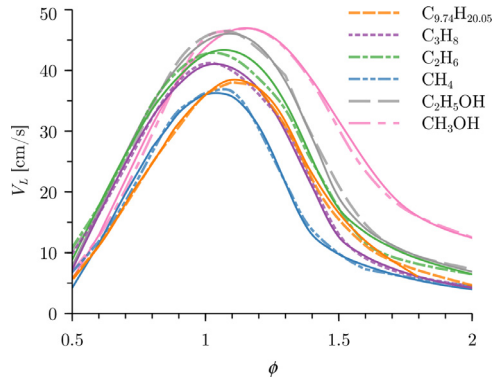

Fig. 3. Laminar burning velocities versus equivalence ratio comparison for the reference mechanism and the 1-step model. Initial conditions for the fuel-air mixtures are $T = 300$K and $P = 1$bar. Solid lines: reference mechanism [8,26]; Dashed lines: present 1-step mechanism.

with $\Gamma(s+1)$ the gamma function. From (23), it is clear that the error on V_L^2 may be exactly corrected through the introduction of a correction function $\mathcal{F} = (V_L^{NC}/V_L^{ref})^2$ in the reaction rate

$$\omega = C_{O_2}^{s/2} C_{C_nH_m}^{s/2} \mathcal{F} K, \tag{24}$$

where $\mathcal{F}$ gathers the change that s_F suffers from passing from lean to rich flames. In practice, we found that defining $\mathcal{F}$ as the product of two ϕ-dependent corrections $\mathcal{F}_i$ defined as

$$\mathcal{F}_i = 1 - \Delta r_{V_L,i}\left[1 - \tanh\left(-\frac{4}{n^0_{O_2}}\frac{\phi - \phi_i}{\Delta\phi_i}\right)\right] \tag{25}$$

is sufficient, with only ($\Delta r_{V_L,i}$, $\Delta\phi_i$, and ϕ_i) as free parameters. The correction $\mathcal{F} = \mathcal{F}_1\mathcal{F}_2$ is defined such as its limit is 1 in the lean limit (no correction) and $(V_L^{NC}/V_L^{ref})^2$ in the rich limit. Separating $\mathcal{F}$ into two separate functions ($\mathcal{F}_1$, $\mathcal{F}_2$) allows to correct both the laminar flame speed value in the rich limit (via $\mathcal{F}_1$) and at stoichiometry (via $\mathcal{F}_2$), a strategy close to the one proposed by Franzelli et al. [8]. For methane/air mixtures the parameters obtained are: $\Delta r_{V_L,1} = 0.17$, $\Delta\phi_1 = 0.131$, $\phi_1 = 0.72$, $\Delta r_{V_L,2} = 0.46$, $\Delta\phi_2 = 0.29$, and $\phi_2 = 1.24$.

The effect of the correction can readily be seen in Fig. 2, showing that the correction function $\mathcal{F}$ in (24) successfully corrects the flame velocity dependence over a wide range of equivalence ratios. A similar agreement is shown in Fig. 3, for a wide variety of fuel-air blends (CH_4, C_2H_6, C_3H_8, CH_3OH, C_2H_5OH, using the San Diego mechanism as a reference [26] and a fuel surrogate for kerosene $C_{9.74}H_{20.05}$ obtaining the values from [8]). The model free parameters (B, T_a, s, $\Delta r_{V_L,1}$, $\Delta\phi_1$, ϕ_1, $\Delta r_{V_L,2}$, $\Delta\phi_2$, and ϕ_2) are provided for each fuel in Supplementary Material.

4. Coupling ignition delay times with laminar flame computations

So far, the mechanism proposed allows to accurately reproduce burnt gas temperature (via the study of Section 2), and premixed combustion characteristics (Section 3). Hereafter, we propose a simple approach allowing to also deal with ignition phenomena as occurring, e.g., in lifted flames.

As duly noted in the literature, chemical time-scales associated with ignition are different from those of premixed flame propagation and tackling both phenomena with a single step is non-trivial [8,27,28]. It is well understood that the ignition process can be well represented by chained reactions building up a radical pool, which eventually will trigger heat-releasing reactions [21,22,29,30]. The exponential character arises from the fact that the reaction rate is proportional to the radical pool concentration, leading to an exponential evolution of radical concentrations [22]. Indeed, such dependence is impossible to obtain with the single-step considered (21) [28]: since no radical carrying the chain-reaction is included [21,30], the rate ω (22) only depends on reactants concentrations which are constant in the first approximation.

Let us now illustrate the difficulty of using single-step chemistry for ignition events. As Carbajal-Carrasco et al. remind in [27], the asymptotic analysis describes the dependence of the ignition delay time or autoignition time as

$$\tau_{ig} \propto \frac{T_u^2}{T_a(T_b - T_u)}\frac{1}{K}. \tag{26}$$

It is then straightforward to derive the Arrhenius constant K_{ig} required for ω in Eq. (22) to obtain accurate ignition times. Unfortunately, because of the different time scales involved, K_{ig} strongly departs from K_{V_L}, the rate optimized in Section 3.

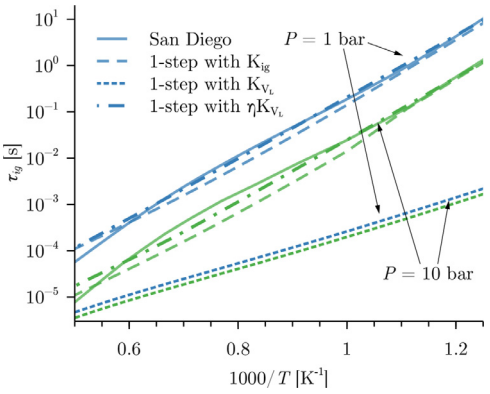

Fig. 4. Ignition delay time versus the inverse of temperature for stoichiometric CH_4-air mixtures at constant volume. Blue lines: initial pressure of 1 bar; Green lines: initial pressure of 10 bar; Solid lines: San Diego mechanism [26]; Dashed lines: single-step mechanism fitted for autoignition conditions (26); Dotted lines: present mechanism without passive scalar correction (24); Dash-dot lines: present mechanism with passive scalar correction (27).

Ignition times predictions, defined as the time when $\partial T/\partial t$ is maximum, were obtained with both K_{ig} and K_{V_L} and they are presented in Fig. 4, confirming the aforementioned point: chemical timescales relative to propagation and ignition are very different, and the rate optimized for propagation leads to ignition times several orders of magnitude shorter than with detailed chemistry. Similar results are obtained with the other considered fuels.

Two main strategies to circumvent this issue may be found in the literature. One strategy consists in fitting two sets of rates (K_{V_L} for flame propagation, K_{ig} for ignition), and switching smoothly between the two based on, e.g., the fresh gases reconstructed temperature [27]. Nonetheless, transitioning between the two can be tricky, and no complex configuration including simultaneously propagation and ignition modes is reported [19,27]. This approach remains appealing, as numerical boundedness of mass fractions is trivial when a single progress variable is considered.

The second strategy is to include a second step [8], thereby providing the additional degree of freedom required. Nonetheless, this is done at the expense of an additional reaction, and of an additional species, whose properties have to be carefully adjusted [27].

In the present work, we intend to keep the best of both approaches by introducing a passive scalar. To account for the exponential property of ignition, we propose the introduction of a scalar variable $\eta \in [0, 1]$, that will play the role of the radical pool precursors, and will serve as an efficiency in Eq. (24)

$$\omega = C_{O_2}^{s_O} C_{C_nH_m}^{s_F} \mathcal{F} K \min(\eta, 1), \tag{27}$$

where the min operator is used to avoid rate acceleration in flame regions, where $\eta > 1$. The scalar is passive in the sense that it does not enter in the mass or energy balance (no mass, no reference energy), but still follows a classical advection-diffusion-reaction equation as

$$\frac{\partial \rho \eta}{\partial t} + \frac{\partial \rho v_\alpha \eta}{\partial x_\alpha} = \frac{\partial}{\partial x_\alpha}\left(\frac{1}{Le_\eta}\frac{\lambda}{c_p}\frac{\partial \eta}{\partial x_\alpha}\right) + \omega_\eta, \tag{28}$$

where the Lewis number can be case-dependent. In the following, we assumed $Le_\eta = 0.18$, a value characteristic of H atom diffusion, but further improvement could be achieved, e.g., by taking into account the molecular composition of the radical pool [22].

The scalar reaction rate ω_η is then written as

$$\omega_\eta = C_M^{s_\eta} B_\eta e^{-\frac{T_{a,\eta}}{T}} (\varepsilon + \eta) \tag{29}$$

where $C_M = \frac{P}{\mathcal{R}T}$ is the total mixture concentration. The presumed form of the reaction rate ω_η is inspired by various analytical studies [21,22,29] and represents both the initiation reaction(s) and chain reactions. The initiation reaction, e.g. $F + O -> R$, is represented by the ε term producing the first radicals even when none is present. The initiation reaction is therefore fundamental: no ignition could occur without it, but its rate is second-order [22,31] on ignition times prediction. The branched-chain reactions are taken into account in (29) via the η term, providing the exponential dependence characteristic of ignition [21,22,29]. The associated Arrhenius rate $B_\eta e^{-\frac{T_{a,\eta}}{T}}$ will provide the ignition temperature dependence, while $C_M^{s_\eta}$ will provide the pressure-dependence, as in third-body reactions. Using asymptotic analysis to solve the coupled global (exothermic) and passive scalar reactions shows that the ignition delay time is proportional to the kinetic parameters as

$$\tau_{ig} \propto \exp\left(\frac{T_a}{T_u}\left[\frac{B}{B_\eta}\frac{T_b - T_u}{T_u}\varepsilon + 1\right]\right) \frac{1}{B_\eta}\log\left(\frac{B_\eta}{B}\frac{T_u^2}{T_a(T_b - T_u)}\frac{0.561}{\varepsilon}\right), \tag{30}$$

showing the role of ε in the temperature dependence of the ignition delay time, which should thus be carefully tuned. Taking into account the analytical solution of η – see more details in the supplemental material – the reaction rate ω_η is finally modified as

$$\omega_\eta = C_M^{s_\eta} B_\eta e^{-\frac{T_{a,\eta}}{T}} \left(\frac{\varepsilon}{\mathcal{F}} + \eta\right) f_\phi, \tag{31}$$

where factor $1/\mathcal{F}$ was introduced to eliminate the rectification made in Equation (24); and f_ϕ is introduced to describe the ϕ dependence of the ignition delay time. Results obtained for methane/air are: $B_\eta = 3 \times 10^{12}$mol/s cm^3, $T_{a,\eta} = 17110$K, $s_\eta = 2$, and $\varepsilon = 1 \times 10^{-7}$. Details on the formula retained for f_ϕ are provided in Supplementary Material but suffice to say, for discussion purposes, that

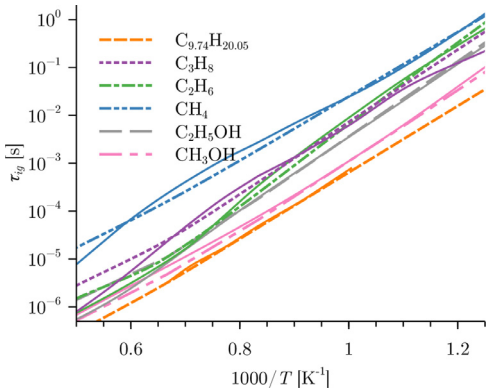

Fig. 5. Ignition delay times versus inverse of temperature comparison for the reference mechanism and the 1-step model. Initial conditions for the stoichiometric fuel-air mixtures at atmospheric pressure $P = 10$bar. Solid lines: reference mechanism [8,26]; Dashed lines: present 1-step mechanism.

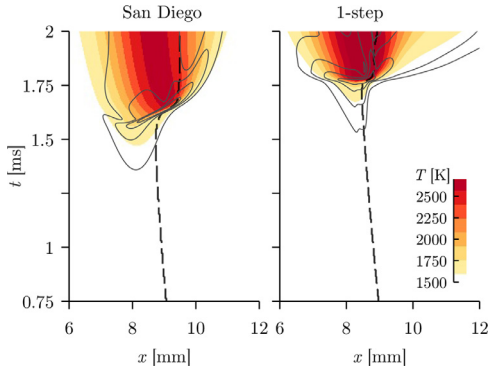

Fig. 6. Transient evolution of one-dimensional CH_4/air mixing layer at atmospheric pressure and initial temperature of 1500K initially located at $x = 10$[mm] with detailed chemistry (left) and current model (right). Black dashed line indicate the location where the mixture is stoichiometric. Solid lines represent isocontours of heat-release rate, while isothermal contours are shown in color.

f_ϕ tends to zero in both rich and lean limits, and has a maximum close to the most-reacting mixture.

Ignition time results using the coupled scalar equation are reported in Fig. 4 (see the ηK_{V_L} curves), showing that the proposed approach is accurate. Since η becomes large in the premixed flame but is clipped to one in the reaction rate (27), results from Fig. 3 remain unaltered. A similar agreement is shown in Fig. 5 for the fuels considered for the study.

The present scalar formulation was fitted for the high-temperature ignition regime, where the chain-branched kinetic path with its associated activation energy suffices to describe the (monotonic) temperature dependence. For low-temperature ignition, some hydrocarbons exhibit negative-temperature-coefficient (NTC) zones [32–34], which will require either increased complexity in the ω_η source term (31), or inclusion of a second scalar for the competing reaction path.

5. Additional validations

This Section aims at validating the chemical model developed in Sections 2–4 in two configurations beyond 1D premixed flames and homogeneous reactors to:

- Verify that the coupling of both reaction rates is satisfying on a simple configuration involving both ignition and propagation.
- Assess the model's capabilities for diffusion flames, even though no particular effort was made in that direction.

5.1. Triple flame

A mixing layer is formed by placing in contact at a given time, two semi-infinite spaces of CH_4 and Air, in quiescent conditions with a high initial temperature ($T_u = 1500$K). Chemical reactions occur as the reactants mix, giving rise to self-ignition in the most reactive zone, and evolving in the formation of two premixed fronts, composed of lean and rich stoichiometries, leaving behind the trailing diffusion flame. These structures, so-called triple flames, are often encountered in several classical applications such as jets of fuel in a hot co-current oxidizer (JHL).

The resulting triple-flame structure can be observed in Fig. 6 through the heat release rate contours and the isothermal surfaces. The single-step model predicts an ignition, defined as the maximum heat-release point, delayed by 10% compared to the detailed mechanism, for a corresponding equivalence ratio about 3% higher thanks to f_ϕ. Note that the Figure does not start at $t = 0$, voluntarily magnifying twice the prediction errors.

These results are highly encouraging, as they show no *footprint* of the efficiency scalar η, while other similar corrections leave clear marks on the flow field (see, e.g., the triple flame in [9]).

5.2. Diffusion flame

Even though the mechanism was derived for premixed combustion, diffusion flame may appear locally in partially premixed combustors. It is therefore of interest to check that the scheme will provide – if not excellent – at least consistent and satisfactory results.

Fig. 7 displays a comparison between the single-step and the detailed chemistry [26] computations of counter-flow diffusion flames under atmospheric conditions. The maximum of temperature, $T_{\max}$, is presented as a function of the strain rate.

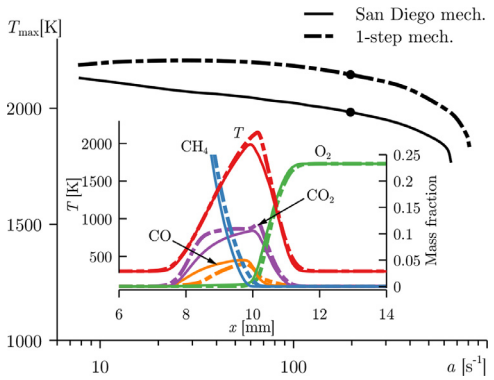

Fig. 7. Variation with strain rate of the maximum temperature in a planar CH_4-air diffusion flame at atmospheric conditions, $T_u = 300$K and $P = 1$bar, and nozzle separation, $L = 0.02$m. Inset shows the temperature and mass fractions profiles of the major species. Solid lines represent the predictions made with San Diego mechanism [26]. Dash-dot lines represent the result made with the present 1-step mechanism. Dots indicates the strain rate at which the inlet profiles were calculated.

The model overpredicts the maximum temperatures in diffusion flames by 8%, a typical value for reduced mechanisms [9]. The measured strain rate is also off by 24% ($a^{SD} = 650$ s^{-1}, $a^{1S} = 807$ s^{-1}). Again this discrepancy is consistent with predictions from existing reduced mechanisms [4,6].

Having pointed out the limitations of the model in the worst conditions, we can conclude that the model provides a satisfactory agreement for diffusion flames, and may be used for partially-premixed combustor simulations.

6. Conclusions and perspectives

A single-step reduced mechanism has been built from an analytical description of the thermochemical equilibrium for a wide-ranging spectrum of fuel-air mixtures, including CH_4, C_2H_6, C_3H_8, CH_3OH, C_2H_5OH, and a fuel surrogate for kerosene $C_{9.74}H_{20.05}$. The formalism proposed offers a simple implementation and does not resort to tabulation. The reaction rate calibration process was able to faithfully reproduce the laminar premixed flame velocity for a wide range of equivalence ratios and initial pressures and temperatures. Note that the single-step formulation leads to trivial boundedness and low stiffness at the expense of species peaks in the flame. It is also the case of most two-step schemes, however, where the second step mainly serves to account for CO equilibrium, here included (along H_2) via varying reaction coefficients.

Coupling with a passive scalar advection-diffusion-reaction equation resulted in excellent induction time estimations, a promising approach towards the simulation of turbulent lifted flames. Similar results could have been obtained introducing an additional intermediate species and reaction instead of η, but the present approach has two major advantages: (i) no minor species is considered, which diminishes both the chemistry stiffness and mesh requirements, and (ii) the passive scalar approach is highly practical numerically. With η being mostly decoupled from the other equations, the simulation stability is fairly insensitive to η. For example, boundedness is very important for minor species (to avoid, e.g. mass defects or simulation crashes), while it has absolutely no effect for η, which can safely be clipped when out-of-bound.

Declaration of Competing Interest

The authors declare that they have no known competing financial interests or personal relationships that could have appeared to influence the work reported in this paper.

Acknowledgments

Arnaud Mura and Antonio Luis Sánchez are gratefully acknowledged for fruitful discussions regarding hydrocarbon single-step chemistry models. We also acknowledge support from the MALBEC ANR project ANR-20-CE05-0009, and the French Defense Agency. Centre de Calcul Intensif d'Aix-Marseille is acknowledged for granting access to its high performance computing resources.

Supplementary material

1. The extension of Section 2 to arbitrary partially oxygenated fuels CnHmOp.
2. Derivation of the analytical solution of η (30).
3. Fitting procedure: the CH_4 example.
4. The parameters derived in Sections 3 and 4, for CH_4, C_2H_6, C_3H_8, CH_3OH, C_2H_5OH, and a fuel surrogate for kerosene $C_{9.74}H_{20.05}$.

References

[1] P. Dagaut, M. Cathonnet, The ignition, oxidation, and combustion of kerosene: a review of experimental and kinetic modeling, Prog Energy Combust Sci 32 (1) (2006) 48–92.
[2] S. Lam, D. Goussis, The csp method for simplifying kinetics, Int. J. Chem. Kinet. 26 (4) (1994) 461–486.

[3] W. Jones, S. Rigopoulos, Reduced chemistry for hydrogen and methanol premixed flames via rcce, Combust. Theor. Model. 11 (5) (2007) 755–780.

[4] A. Er-Raiy, Z. Bouali, J. Réveillon, A. Mura, Optimized single-step (oss) chemistry models for the simulation of turbulent premixed flame propagation, Combust. Flame 192 (2018) 130–148.

[5] U. Maas, S. Pope, Implementation of simplified chemical kinetics based on intrinsic low-dimensional manifolds, Symp. (Int.) Combust. 24 (1) (1992) 103–112. Twenty-Fourth Symposium on Combustion

[6] E. Fernández-Tarrazo, A.L. Sánchez, A. Linan, F.A. Williams, A simple one-step chemistry model for partially premixed hydrocarbon combustion, Combust. Flame 147 (1–2) (2006) 32–38.

[7] N. Peters, B. Rogg, Reduced kinetic mechanisms for applications in combustion systems, volume 15, Springer Science & Business Media, 2008.

[8] B. Franzelli, E. Riber, M. Sanjosé, T. Poinsot, A two-step chemical scheme for kerosene–air premixed flames, Combust. Flame 157 (7) (2010) 1364–1373.

[9] P. Boivin, C. Jiménez, A.L. Sánchez, F.A. Williams, An explicit reduced mechanism for H_2–air combustion, Proc. Combust. Inst. 33 (1) (2011) 517–523.

[10] M. Cailler, N. Darabiha, B. Fiorina, Development of a virtual optimized chemistry method. application to hydrocarbon/air combustion, Combust. Flame 211 (2020) 281–302.

[11] R. Sankaran, E.R. Hawkes, J.H. Chen, T. Lu, C.K. Law, Structure of a spatially developing turbulent lean methane–air bunsen flame, Proc. Combust. Inst. 31 (1) (2007) 1291–1298.

[12] Z.M. Nikolaou, J.-Y. Chen, N. Swaminathan, A 5-step reduced mechanism for combustion of co/h2/h2o/ch4/co2 mixtures with low hydrogen/methane and high h2o content, Combust. Flame 160 (1) (2013) 56–75.

[13] A.D. Weiss, A.L. Sánchez, F.A. Williams, Accuracies of reduced mechanisms for predicting acoustic combustion instabilities, Combust. Flame 209 (2019) 405–407.

[14] P. Boivin, C. Jiménez, A.L. Sánchez, F.A. Williams, A four-step reduced mechanism for syngas combustion, Combust. Flame 158 (6) (2011) 1059–1063.

[15] P. Boivin, A.L. Sánchez, F.A. Williams, Four-step and three-step systematically reduced chemistry for wide-range H_2–air combustion problems, Combust. Flame 160 (1) (2013) 76–82.

[16] P. Boivin, F.A. Williams, Extension of a wide-range three-step hydrogen mechanism to syngas, Combust. Flame 196 (2018) 85–87.

[17] B. Varatharajan, M. Petrova, F. Williams, V. Tangirala, Two-step chemical-kinetic descriptions for hydrocarbon–oxygen-diluent ignition and detonation applications, Proc. Combust. Inst. 30 (2) (2005) 1869–1877.

[18] K. Akihama, Y. Takatori, K. Inagaki, S. Sasaki, A.M. Dean, Mechanism of the smokeless rich diesel combustion by reducing temperature, SAE Trans. (2001) 648–662.

[19] A. Misdariis, O. Vermorel, T. Poinsot, A methodology based on reduced schemes to compute autoignition and propagation in internal combustion engines, Proc. Combust. Inst. 35 (3) (2015) 3001–3008.

[20] F. Mauss, N. Peters, B. Rogg, F. Williams, Reduced Kinetic Mechanisms for Premixed Hydrogen Flames, in: Reduced Kinetic Mechanisms for Applications in Combustion Systems, Springer, 1993, pp. 29–43.

[21] L. Veggi, P. Boivin, Explicit formulation of the reactivity of hydrogen, methane and decane, Combust. Flame 162 (3) (2015) 580–585.

[22] P. Boivin, A. Sánchez, F. Williams, Analytical prediction of syngas induction times, Combust. Flame 176 (2017) 489–499.

[23] T. Poinsot, D. Veynante, Theoretical and numerical combustion, RT Edwards, Inc., 2005.

[24] W.C. Reynolds, The element potential method for chemical equilibrium analysis: implementation in the interactive program stanjan, Technical Rept. (1986).

[25] D.G. Goodwin, H.K. Moffat, R.L. Speth, Cantera: an object-oriented software toolkit for chemical kinetics, thermodynamics, and transport processes, Caltech, Pasadena, CA 124 (2009).

[26] Chemical-kinetic mechanisms for combustion applications, (web.eng.ucsd.edu/mae/groups/combustion/mechanism.html) V. 2016-12-14.

[27] L.A. Carbajal-Carrasco, Z. Bouali, A. Mura, Optimized single-step (oss) chemistry for auto-ignition of heterogeneous mixtures, Combust. Flame 227 (2021) 11–26.

[28] M.L. Boursicaud, L.A. Carbajal-Carrasco, Z. Bouali, A. Mura, Optimized two-step (ots) chemistry models for the simulation of turbulent premixed flame propagation and ignition, Under consideration for publication (2022).

[29] C. Treviño, F. Mendez, Reduced kinetic mechanism for methane ignition, Proc. Combust. Inst. 24 (1) (1992) 121–127.

[30] D.J. Diamantis, D.C. Kyritsis, D.A. Goussis, The reactions supporting or opposing the development of explosive modes: auto-ignition of a homogeneous methane/air mixture, Proc. Combust. Inst. 35 (1) (2015) 267–274.

[31] C. Treviño, F. Solorio, Asymptotic analysis of the high-temperature ignition of co/h_2/o_2 mixtures, Combust. Flame 86 (3) (1991) 285–295.

[32] N. Peters, G. Paczko, R. Seiser, K. Seshadri, Temperature cross-over and non-thermal runaway at two-stage ignition of n-heptane, Combust. Flame 128 (1–2) (2002) 38–59.

[33] U. Pfahl, K. Fieweger, G. Adomeit, Self-ignition of diesel-relevant hydrocarbon-air mixtures under engine conditions, in: Symposium (international) on combustion, volume 26, Elsevier, 1996, pp. 781–789.

[34] P. Zhang, W. Ji, T. He, X. He, Z. Wang, B. Yang, C.K. Law, First-stage ignition delay in the negative temperature coefficient behavior: experiment and simulation, Combust. Flame 167 (2016) 14–23.